THE JOURNAL OF PHYSICAL CHEMISTRY B

Article

pubs.acs.org/JPCB

Proton Conduction in Water Ices under an Electric Field

Giuseppe Cassone,[†,‡,§,∥] Paolo V. Giaquinta,[†] Franz Saija,[*,‡] and A. Marco Saitta[§,∥]

[†] Dipartimento di Fisica e di Scienze della Terra, Università degli Studi di Messina, Contrada Papardo, 98166 Messina, Italy

[‡]CNR-IPCF, Viale Ferdinando Stagno d'Alcontres 37, 98158 Messina, Italy

[§]UPMC Univ Paris 06, UMR 7590, IMPMC, F-75005 Paris, France

[∥]CNRS, UMR 7590, IMPMC, F-75005 Paris, France

ABSTRACT: We report on a first-principles study of the effects produced by a static electric field on proton conduction in ordinary hexagonal ice (phase I_h) and in its proton-ordered counterpart (phase XI). We performed ab initio molecular dynamics simulations of both phases and investigated the effects produced by the field on the structure of the material, with particular attention paid to the phenomenon of proton transfer. We observed that in ice I_h molecules start to dissociate for field intensities around 0.25 V/Å, as in liquid water, whereas fields stronger than 0.36 V/Å are needed to induce a permanent proton flow. In contrast, in ice XI, electric fields as intense as 0.22 V/Å are already able to induce and sustain, through correlated proton jumps, an ionic current; this behavior suggests, somewhat counterintuitively, that the ordering of protons favors the autoprotolysis phenomenon. However, the same is not true for static conductivities. In fact, both crystalline phases show an ohmic behavior in the conduction regime, but the conductivity of ice I_h turns out to be larger than that of ice XI. We finally discuss the qualitative and quantitative importance of the conspicuous concentration of ionic defects generated by intense electric fields in determining the value of the conductivity, also through a comparison with the experimental data available for saline ices.

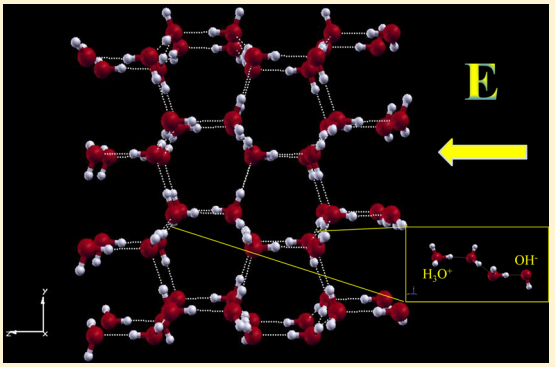

I. INTRODUCTION

Water is one of the most abundant substances on Earth and likely is the most studied compound in condensed matter physics. It has a very rich phase diagram with at least 16 crystalline phases and three amorphous phases.[1] However, despite the huge experimental evidence and theoretical results which have accumulated so far, some structural and dynamical properties of the liquid and solid phases of water are not yet fully understood.[1,2]

Of paramount relevance is the phenomenon of molecular dissociation and the related phenomenon of proton transfer. This process, which in liquid water is known as (auto)-protolysis, plays a crucial role in many disparate domains, from neurobiology to electrolytic batteries and hydrogen-based technology.[3,4] At standard conditions this phenomenon is as rare as it is fundamental because, among other things, it represents the basis of the definition of the pH concept via the well-known reaction

$$2H_2O \rightleftharpoons OH^- + H_3O^+ \quad (1)$$

where two water molecules ionize by transferring one proton. Although the way in which this process, known as the Grotthuss mechanism[5], occurs along hydrogen-bonded chains of water molecules is phenomenologically clear since the 1800s, a coherent theoretical framework that explains in detail all the relevant aspects characterizing the protolysis and the proton-transfer mechanism is still missing.

In principle, the study of the hydrogen bond (H-bond) network of solid water phases is easier than that of the liquid phase. In this respect, ice phases are good candidates in which to study both the static and dynamic properties of the proton-transfer mechanism. At ambient conditions, the stable crystalline phase is ice I_h, whose molecules are positionally arranged in an hexagonal lattice while being orientationally disordered (i.e., the proton sublattice is randomly distributed). When KOH-doped ice I_h is cooled to a temperature of 72 K, it is possible to obtain its proton-ordered counterpart (ice XI),[6,7] whose molecules are oriented along the *c*-axis (i.e., the *z*-component of the dipole moments is everywhere positive). In the I_h-to-XI first-order phase transition, the KOH hydroxide ions catalyze the rearrangement of H bonds, via defects formation, which leads to an enhanced molecular mobility. In this way, water molecules exploit a more stable condition by reducing the original symmetry of the crystalline phase from hexagonal to orthorhombic, thus giving rise to the ferroelectric ice XI phase. The ordering of the proton sublattice obviously affects the properties of the material and, in particular, the electrical polarizability and the conductivity. In this respect, ice can be described as a "protonic semiconductor". Indeed, ionic defects (i.e., hydronium and hydroxide) together with Bjerrum

Received: March 1, 2014
Revised: April 1, 2014
Published: April 1, 2014

 © 2014 American Chemical Society dx.doi.org/10.1021/jp5021356 | *J. Phys. Chem. B* 2014, 118, 4419−4424

orientational defects are responsible for electrical transport processes in ice phases.[1]

Recently, some relevant efforts have been made to understand the proton-transfer mechanism so as to fill the gap between theory and experiment.[8−10] One of the main difficulties is associated with the extremely rare nature of the protolysis phenomenon. In this respect, Saitta and co-workers[11] have shown, in an ab initio study of water dissociation, that it is possible to stimulate the proton-transport process and to investigate it in a systematic fashion by applying an external electric field.

In this manuscript we extend this computational approach to crystalline phases of water. In fact, the peculiar symmetries of I_h and XI ices allow a qualitative and quantitative investigation of the entropic and energetic contributions to the proton-transfer phenomenon. We use the Car−Parrinello technique[12] to determine the energetic profiles of the molecular dissociation phenomenon and monitor some dynamic properties of the system, with particular emphasis on proton transfer along H-bonded water molecules. We also carry out some comparisons with the experimental results available in ices with high defect concentrations.

The manuscript is structured as follows. After the Introduction, we discuss the Computational Methods. The Results and Discussion section is followed by Conclusions.

II. COMPUTATIONAL METHODS

By using the Car−Parrinello approach,[12] we performed a series of static and dynamic ab initio simulations on two ice phases, i.e., ice I_h and ice XI, under the effect of intense electric fields, applied along the *c* cell parameter, to study the phenomenon of ionic conduction. All data were obtained using the software suite Quantum ESPRESSO[13] for ab initio electronic structure calculations within which it is possible to handle macroscopic polarization and finite electric fields by exploiting the modern theory of polarization (Berry phases).[14,15]

Our systems were composed of 64 H_2O molecules arranged in an orthorhombic cell with parameters a = 9.05 Å, b = 15.67 Å, and c = 14.87 Å. To test potential size effects along the field direction, we also performed some numerical calculations on samples with 96 and 128 molecules, built with a *c* cell parameter whose values were 22.31 and 29.74 Å, respectively. Periodic boundary conditions were applied in all simulations.

The positions occupied by the oxygen atoms are the same in the two ice structures; however, the arrangements of the hydrogen atoms differ significantly. In fact, the orientations of the molecules that compose the I_h phase, while complying with the Bernal−Fowler ice rules,[16] are disordered, giving rise to a $P6_3/mmc$ symmetry; in contrast, those belonging to the ice XI phase are orientationally ordered and form a crystalline structure that belongs to the $Cmc2_1$ space group.

The calculation of the molecular dissociation energy profiles is performed via electronic minimization by using, sequentially, the Gram−Schmidt and Davidson algorithms. In the following, we shall refer to such total energy profiles as "single", "double", or "triple" barriers according to the number of protons involved in the jump from their original sites. In the case of a double (triple) barrier, in which two (three) protons of H-bonded molecules simultaneously move, the protons were selected in this way: one belonging to the donor and one to the acceptor molecule, which in turn becomes the donor, and so on. We verified that the single- and double-barrier cases cannot account for a potentially alternative scenario which may justify the jump of a proton on the energetic side. Hence, we limit our discussion to the triple-barrier profiles that are displayed in Figure 1, whose inset also shows three snapshots of the

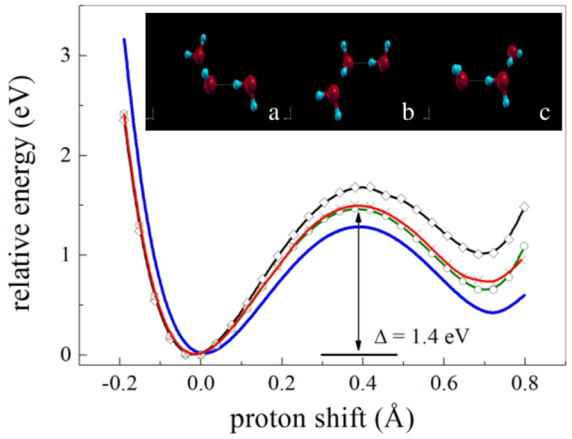

Figure 1. Relative energies corresponding to proton shifts of a given distance along an H-bonded chain formed by three water molecules, for an electric field intensity of 0.36 V/Å, in a system with 64 molecules; the solid blue line refers to ice XI, whereas the other curves refer to ice I_h and were generated using three different molecular configurations that are shown in the inset: (a) configuration of three water molecules present in both I_h and XI structures leading to the blue curve and green curve with circles, respectively, upon displacing protons as discussed in the text; (b) configuration of three water molecules in ice I_h leading to the red line with crosses; (c) configuration of three water molecules in ice I_h leading to the black line with diamonds.

molecular configurations involved in the calculations. These configurations were chosen because the molecular dipole moments are partially aligned with the field direction (positive *z* component). In particular, the configuration shown in Figure 1a is the same as the one used in the ferroelectric case and is obviously the most favorable one for proton transfer in the arrangement of the present numerical experiment. Barriers along the selected reaction coordinates were calculated via single, double, or triple proton shift(s) of 0.038 Å.

The dynamic ab initio simulations were performed at the nominal temperature of 300 K which, according to the literature,[17−19] corresponds to a real temperature of about 250 K. The effect of the electric field was explored for intensities less than or equal to 0.36 V/Å, with a step increment of approximately 0.036 V/Å, which leads to a total simulation time of more than 10 ps (for each value of the field intensity the duration of the simulation was at least 1 ps). Several dynamic runs were conducted also for stronger electric fields (up to about 0.73 V/Å) to obtain a full description of the current−voltage diagram of ice I_h. The fictitious electronic mass was set at a value of 300 au, with a cutoff energy ranging between 25 and 35 Ry and a cutoff energy for the charge density of 200−280 Ry. These values made it possible to adopt a Car−Parrinello time step of about 0.1 fs. We used the Perdew−Burke−Ernzerhov (PBE) functional,[20] which belongs to the generalized gradient approximation (GGA), as an exchange and correlation functional because of its well-known reliability when dealing with aqueous systems.[11,21−23] The electronic interaction with the nuclei was described through ultrasoft pseudopotentials (USPP), and the ion dynamics was carried out in the *NVT* ensemble, using the Verlet algorithm and

dx.doi.org/10.1021/jp5021356 | J. Phys. Chem. B 2014, 118, 4419−4424

Nosé–Hoover thermostat at a frequency of 13.5 THz. Protons were treated as classical particles. Although nuclear quantum effects do certainly play a role in proton barriers and diffusion, we focused more on relative values emerging from a comparison between proton-ordered and proton-disordered phases.

The conductivities were obtained by exploiting Ohm's law. The current intensity is related to the number of charge carriers and to the time interval Δt considered. The former quantity was obtained from the simulation data by calculating the number of protons ΔN traveling through a section area of the simulation box orthogonal to the electric field direction. The potential difference can be obtained by considering the strength E of the electric field and the length c of the simulation box along which the field is applied. Finally, by taking into account the value of the section area orthogonal to the field direction, the conductivity can be estimated as

$$\sigma = \frac{\Delta N \cdot q}{(E \cdot c) \cdot \Delta t} \frac{c}{a \cdot b} \tag{2}$$

where q is the elementary charge and a, b, and c are the cell parameters corresponding to the x-, y-, and z-axes.

III. RESULTS AND DISCUSSION

In liquid water, molecules start to dissociate for field intensities of about 0.25 V/Å,[11,24−26] while a net proton flow is observed along the z-direction for intensity values above 0.36 V/Å.[11] We found that the same thresholds apply to ice I_h which, in this respect, behaves as liquid water; this finding is not particularly surprising because the dipole moments orientational distributions are similar in both phases. In contrast, in ice XI, the angular symmetry is broken in that the z-component of the dipole moments is, on average, positive, a condition that leads to the emergence of an internal electric field (ferroelectric phase). As a result, the electrostatic coupling with the external field is significantly enhanced. Correspondingly, the first dissociation events are observed for field intensities in the 0.18–0.22 V/Å range, at which threshold protons also start to flow in a sustained way. The simultaneous onset of such two phenomena is a distinguishing feature of ice XI as compared with the two-stage behavior observed in ice I_h and liquid water.

To investigate the mechanism underlying molecular dissociation and proton transfer we first performed a series of "static" calculations of the potential energy profiles, obtained in both ice structures at 0 K after displacing–along the field direction and by the same distance from their original sites–up to three protons while keeping the oxygen atoms fixed at their original positions: one selected proton belonging to a molecule which possesses at least one hydrogen atom which can be shifted along the positive direction of the field, a proton covalently bonded to a first-neighbor oxygen atom, and one more proton belonging to a molecule that is hydrogen-bonded to the second one. In ice XI all choices are equivalent because they at most differ for the orientation of the central molecule with respect to the other two; in contrast, in ice I_h, there are only three configurations of three "wired" molecules such that on each molecule it is possible to find at least one hydrogen atom, bonding with a neighboring oxygen, which can be displaced along the field direction (i.e., along the positive z-axis). The results of these static calculations are shown in Figure 1 for a field strength of 0.36 V/Å, which corresponds to the proton conduction regime. We see that, in addition to the energy minimum associated with the unperturbed configuration, all the curves show a secondary minimum at the distance where the displaced proton might covalently bond with the nearby oxygen atom. However, even for very high field strengths this minimum is not deep enough to justify, on a mere energetic basis, the proton transfer and the corresponding formation of an ionic pair. Hence, a scenario in which oxygen atoms are held fixed while protons move along a "chain" does not suffice to explain the dissociation of a water molecule. However, note that, notwithstanding the failure of our constrained model calculation in accounting for the energetics of the proton transfer, the height of the barrier separating the two minima in the most favorable I_h configuration (∼1.4 eV) turns out to be in fair agreement with the available experimental data for the activation energy of the process leading to the formation of an ionic pair.[1]

The role of the network formed by the oxygen atoms in assisting, locally, the proton-transfer event can be elucidated by dynamical simulations. We observed that the external field produces a notable effect in that it "flattens" the planes parallel to its direction. This phenomenon is more clearly resolved in ice XI, as shown in the inset of Figure 2, and can be attributed

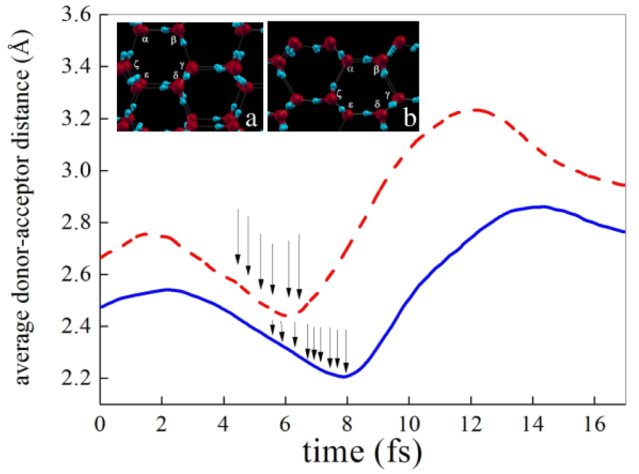

Figure 2. Donor–acceptor distances during the first ionization events (identified by the arrows) in a system with 64 molecules: the solid blue line refers to ice XI while the dashed red line refers to ice I_h. The inset shows (a) the standard ice XI structure and (b) the field-induced planes flattening, with pertinent angles labeled as Greek letters. In panel a, $\alpha = \beta = \gamma = \delta = \varepsilon = \zeta = 109.45°$. In panel b, $\alpha = 113.2°$, $\beta = 112.9°$, $\gamma = 102.3°$, $\delta = 114.8°$, $\varepsilon = 114.8°$, and $\zeta = 102.4°$, a configuration which exhibits a shortening of the in-plane intermolecular lengths.

to a sort of "pressure"[11,27] exerted by the applied field which forces the mutual alignment of molecular dipole moments. The resulting polarization effect ultimately enhances the electrostatic coupling between the molecular dipole moments and the external field in a powered manner. In ice I_h the flattening of the planes was not observed as clearly as in the ferroelectric case because a larger energy is needed, on average, to align disordered dipole moments with the field direction. In ice XI, we further observed the alignement of the oxygen planes perpendicular to the applied field: molecular orientations are restored after a diffusion process has taken place via a Grotthuss mechanism,[5] which causes an inversion of the involved dipole moments.

dx.doi.org/10.1021/jp5021356 | J. Phys. Chem. B 2014, 118, 4419–4424

As a consequence of the flattening process described above, the mutual distances between oxygen atoms decrease: this structural rearrangement enhances the probability of occurrence of correlated proton jumps which enable the phenomenon of diffusion. Correspondingly, the potential barrier that protons must overcome when migrating from a donor to an acceptor molecule, following the formation of a Zundel complex ($H_3O^+ + H_2O \rightarrow H_5O_2^+$), decreases[28] and attains its minimum value for an oxygen−oxygen distance of about 2.4 Å.[29,30] In both crystalline structures we observed a shortening of the hydrogen bond chain whenever an ionization event occurred (see Figure 2). This behavior is coherent with the phenomenology observed by Hassanali and co-workers[31] in liquid water and confirms that the diffusion event is the result of a highly cooperative molecular motion. When the H_3O^+−H_2O distance decreases, the proton localization probability decreases as well and, correspondingly, the proton-transfer probability increases along the hydrogen bond chain.[28] The process is Zundel-to-Zundel type and is mediated by water molecules as in the liquid phase:[31] when an H_3O^+ ion gets sufficiently close to an H_2O molecule, a Zundel ion forms and, after multiple exchanges of the ionic roles between the two entities, the complex eventually propagates with a Grotthuss-type dynamics.

As soon as a sustained proton diffusion has been activated, both ices display an ionic ohmic behavior (see Figure 3), which

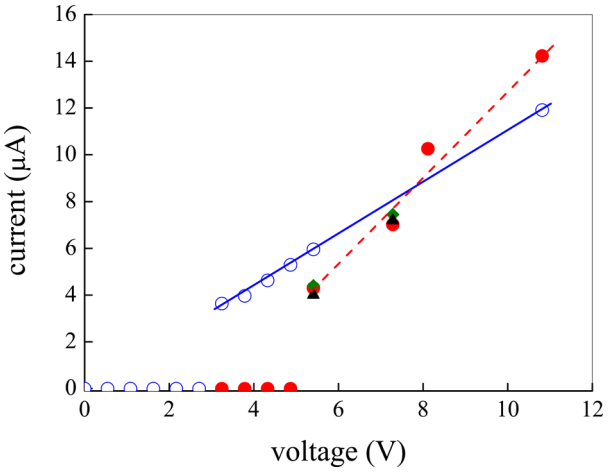

Figure 3. Ionic current−voltage characteristic for an orthorhombic cell with edges a = 9.05 Å, b = 15.67 Å, and c = 14.87 Å: (solid circles) samples of ice I_h with 64 molecules; (open circles) samples of ice XI with 64 molecules; (diamonds) samples of ice I_h with 96 molecules; (triangles) samples of ice I_h with 128 molecules (lines are a guide for the eye).

has been observed experimentally in the common phase of ice for voltages up to about 10 V.[32] We calculated the static conductivities of ice I_h and ice XI to be 6.9 and 5.8 Ω^{-1} cm^{-1}, respectively. Indeed, these values are many orders of magnitude higher than those obtained experimentally for *pure* crystalline phases of ice which, however, refer to significantly lower field strengths (10^{-10}−10^{-4} V/Å).[32,33] Following Jaccard, who explained proton mobility in ices in terms of defects,[34] we attribute the discrepancy between our estimates and the experimental data to the widely varying concentrations of ionic defects that are generated by the applied field. Moreover, as shown in Figure 3, no significant and systematic differences emerge between the estimates obtained with different sample sizes.

Table 1 shows the percent fractions of defects that are present in the two simulated crystalline structures for increasing

Table 1. Percent Fractions of Ionic Defects Induced in Ice I_h and Ice XI by Increasing Electric-Field Strength

electric field strength (V/Å)	ice I_h	ice XI
0.22		3%
0.25		5%
0.29		6%
0.33		8%
0.36	8%	9%
0.47	11%	
0.55	13%	
0.73	19%	16%

field strengths; the values corresponding to the most intense applied field (0.73 V/Å) range between 16% and 19%. Such concentrations are actually typical of doped materials. Grimm et al.[35] investigated ice I_h doped with $CaCl_2$ and other salts for increasing molarities (1, 2.25, 3.14, and 3.96 M), over a wide range of temperatures. In fact, the concentration of defects generated via the formation of HCl (see Table 2) with a salt

Table 2. Percent Fractions of Defects Present in Ice I_h Doped with Increasing Molarities of $CaCl_2$[35]

salt molarity	fraction of ionic defects
1	4.0%
2.25	8.4%
3.14	11.6%
3.96	14.4%

molarity of 3.96 is comparable with the values displayed in Table 1. The estimates of the percent fractions of defects present in experimentally heavily doped ices were obtained by considering a one-to-one correspondence between doping and defect levels, as shown in ref 36. Upon extrapolating the low-temperature conductivity data of this material outside the sampled range, i.e., well above the eutectic point, up to the temperature of our numerical experiments, one would recover values of the same order or even larger than those reported above for nondoped ice.

Another comparison can be made with the conductivity of KOH-doped ice I_h as measured by Zaretskii et al.[37] with alternating currents. However, beyond a temperature threshold of about 200 K, such a frequency-dependent conductivity does no longer depend in an appreciable way on the frequency of the applied field. For instance, in 1 M KOH-doped ice I_h, where the fraction of ionic defects is about 2%, the conductivity measured by Zaretskii et al. at 283 K was about 10^{-1} Ω^{-1} cm^{-1}. Again, the discrepancy between this value and our results for the static conductivities of nondoped ices can be largely accounted for by the different temperatures and defect concentrations. Indeed, upon extrapolating the experimental conductivity curves, we recover values whose orders of magnitude are comparable with the data extracted by the present simulations.

IV. CONCLUSIONS

In this article we investigated the effect of proton ordering on the transport properties of water ices I_h and XI under intense

dx.doi.org/10.1021/jp5021356 | J. Phys. Chem. B 2014, 118, 4419−4424

electric fields. We found that the enhanced coupling between the dipole moments and the internal electric field makes it simpler for water molecules to dissociate in the ferroelectric phase than in ice I_h. On the other side, restoring the dipole moments distribution after a proton has migrated via the Grotthuss mechanism is less problematic in ice I_h than in ice XI, where all molecular dipoles need to be retilted in order for another proton to be transferred along a given path. This leads to a higher static conductivity of common ice as compared with that of its proton-ordered counterpart. This "ambivalent" role played by proton (dis)order is an unexpected and so far unreported feature of water dissociation and proton conduction in ices.

We conclude that orientational order favors, on the energetic side, the dissociation of water molecules but hinders the proton diffusion which is instead promoted and amplified by proton disorder with its associated contribution to the entropy of the material. Moreover, the fact that the dissociation and current thresholds are the same in liquid water and in ice I_h suggests that the stability of the molecular interactions does not affect the conductivity and that the symmetry of the problem plays a crucial role in the protolysis as well as in the proton-transfer phenomena.

AUTHOR INFORMATION

Corresponding Author

*E-mail: saija@ipcf.cnr.it.

Notes

The authors declare no competing financial interest.

ACKNOWLEDGMENTS

We acknowledge the IDRIS Supercomputing Facility for CPU time (x2013091387). G.C. thanks IMPMC and UPMC for their scientific hospitality during several stretches of few months each.

REFERENCES

(1) Petrenko, V. F.; Whitworth, R. W. *Physics of Ice*; Oxford University Press: Oxford, U.K., 1999.

(2) Debenedetti, P. G. *Metastable Liquids: Concepts and Principles*; Princeton University Press: Princeton, NJ, 1996.

(3) Kaila, K.; Ransom, B. R. *pH and Brain Function*; Kaila, K., Ransom, B.R., Eds.; Wiley: New York, 1998.

(4) Zoulias, E. I.; Lymberoupolos, N. *Hydrogen-Based Autonomous Power Systems*; Springer: London, 2008.

(5) Grotthuss, C. J. T. Sur la décomposition de l'eau et des corps qu'elle tient en dissolution à l'aide de l'électricité galvanique. *Ann. Chim. (Paris, Fr.)* **1806**, *LVIII*, 54−74.

(6) Tajima, Y.; Matsuo, B. R.; Suga, T. H. Phase Transition in KOH-Doped Hexagonal Ice. *Nature (London, U.K.)* **1982**, *299*, 810.

(7) Umemoto, K.; Wentzcovitch, R. M.; Baroni, S.; de Gironcoli, S. Anomalous Pressure-Induced Transition(s) in Ice XI. *Phys. Rev. Lett.* **2004**, *92*, 105502.

(8) Hassanali, A.; Giberti, F.; Cuny, J.; Kühne, T. D.; Parrinello, M. Proton Transfer Through the Water Gossamer. *Proc. Natl. Acad. Sci. U.S.A.* **2013**, *110*, 142237−14242.

(9) Cwiklik, L.; Buch, V. Hydroxide Trapped in the Interior of Ice: A Computational Study. *Phys. Chem. Chem. Phys.* **2009**, *11* (9).

(10) Tuckerman, M. E.; Chandra, A.; Marx, D. Structure and Dynamics of OH^-(aq). *Acc. Chem. Res.* **2006**, *39*, 151.

(11) Saitta, A. M.; Saija, F.; Giaquinta, P. V. *Ab initio* Molecular Dynamics Study of Dissociation of Water Under an Electric Field. *Phys. Rev. Lett.* **2012**, *108*, 207801.

(12) Car, R.; Parrinello, M. Unified Approach for Molecular Dynamics and Density-Functional Theory. *Phys. Rev. Lett.* **1985**, *55*, 2471.

(13) Giannozzi, P.; et al. QUANTUM ESPRESSO: A Modular and Open-Source Software Project for Quantum Simulation of Materials. *J. Phys.: Condens. Matter* **2009**, *21*, 395502.

(14) Berry, M. V. Quantal Phase Factors Accompanying Adiabatic Changes. *Proc. R. Soc. London, Ser. A* **1984**, *392*, 45.

(15) Umari, P.; Pasquarello, A. *Ab initio* Molecular Dynamics in a Finite Homogeneous Electric Field. *Phys. Rev. Lett.* **2002**, *89*, 157602.

(16) Bernal, J. D.; Fowler, R. H. A Theory of Water and Ionic Solution, with Particular Reference to Hydrogen and Hydroxyl Ions. *J. Chem. Phys.* **1933**, *1*, 515.

(17) Del Buono, G. S.; Rossky, P. J.; Schnitker, J. Model Dependence of Quantum Isotope Effects in Liquid Water. *J. Chem. Phys.* **1991**, *95*, 3728.

(18) Allesch, M.; Schwegler, E.; Gygi, F.; Galli, G. First Principles Simulations of Rigid Water. *J. Chem. Phys.* **2004**, *120*, 5192.

(19) Grossman, J. C.; Schwegler, E.; Draeger, E. W.; Gygi, F.; Galli, G. Towards an Assessment of the Accuracy of Density Functional Theory for First Principles Simulations of Water. *J. Chem. Phys.* **2004**, *120*, 300.

(20) Perdew, J. P.; Burke, K.; Ernzerhof, M. Generalized Gradient Approximation Made Simple. *Phys. Rev. Lett.* **1996**, *77*, 3865−3868; *Phys. Rev. Lett.* **1997**, *78*, 1396−1396.

(21) Fiolhais, C.; Nogueira, F.; Marques, M. *A Primer in Density Functional Theory*; Springer-Verlag: Berlin Heidelberg, Germany, 2010.

(22) Santra, B.; Klimes, J.; Alfé, D.; Tkatchenko, A.; Slater, B.; Michaelides, A.; Car, R.; Sheffer, M. Hydrogen Bonds and van der Waals Forces in Ice at Ambient and High Pressure. *Phys. Rev. Lett.* **2011**, *107*, 185701.

(23) Hamann, D. R. H_2O Hydrogen Bonding in Density-Functional Theory. *Phys. Rev. B* **1997**, *55*, R10157−R10160.

(24) Stuve, E. M. Ionization of Water in Interfacial Electric Fields: An Electrochemical Overview. *Chem. Phys. Lett.* **2012**, *519*−*520*, 1.

(25) Hammadi, Z.; Descoins, M.; Salanon, E.; Morin, R. Proton and Light Ion Nanobeams from Field Ionization of Water. *Appl. Phys. Lett.* **2012**, *101*, 243110.

(26) Geissler, P. I.; Dellago, C.; Chandler, D.; Hutter, J.; Parrinello, M. Autoionization in Liquid Water. *Science* **2001**, *291*, 2121−2124.

(27) Schwegler, E.; Galli, G.; Gygi, F.; Hood, R. Q. Dissociation of Water under Pressure. *Phys. Rev. Lett.* **2001**, *87*, 265501.

(28) Marx, D. Proton Transfer 200 Years after von Grotthuss: Insights from *Ab initio* Simulations. *ChemPhysChem* **2006**, *7*, 1848−1870.

(29) Xie, Y.; Remington, R. B.; Schaefer, H. F. The Protonated Water Dimer: Extensive Theoretical Studies of $H_5O_2^+$. *J. Chem. Phys.* **1994**, *101*, 4878.

(30) Tuckerman, M. E.; Marx, D.; Klein, M. L.; Parrinello, M. On the Quantum Nature of the Shared Proton in Hydrogen Bonds. *Science* **1997**, *275*, 817−820.

(31) Hassanali, A.; Prakash, M. K.; Eshet, H.; Parrinello, M. On the Recombination of Hydronium and Hydroxide Ions in Water. *Proc. Natl. Acad. Sci. U.S.A.* **2011**, *108*, 20410.

(32) Maidique, M. A.; von Hippel, A.; Westphal, W. B. *Transfer of Protons through Pure Ice in Single Crystals − Part III. The Dielectric Relaxation Spectra of Water, Ice, and Aqueous Solutions and Their Interpretation*; Laboratory for Insulation Research, Massachusetts Institute of Technology, Technical Report 8, 1970.

(33) Liu, B.; Yang, J.; Wang, Q.; Han, Y.; Ma, Y.; Gao, C. Determination of Phase Diagram of Water and Investigation of Electrical Transport Properties of Ices VI and VII. *Phys. Chem. Chem. Phys.* **2013**, *15*, 14364−14369.

(34) Jaccard, C. Thermodynamics of Irreversible Processes Applied to Ice. *Phys. Kondens. Mater.* **1964**, *3*, 99−118.

(35) Grimm, R. E.; Stillman, D. E.; Dec, S. F.; Bullock, M. A. Low-Frequency Electrical Properties of Polycrystalline Saline Ice and Salt Hydrates. *J. Phys. Chem. B* **2008**, *112*, 15382−15390.

(36) Fletcher, N. H. *The Chemical Physics of Ice*; Cambridge Monographs on Physics: Cambridge, U.K., 1970.
(37) Zaretskii, A. V.; Petrenko, V. F.; Chesnakov, V. A. The Protonic Conductivity of Heavily KOH-Doped Ice. *Phys. Status Solidi A* **1988**, *109*, 373.